

Angiotensin II augments renal vascular smooth muscle sGC expression via an AT₁R - FoxO transcription factor signaling axis

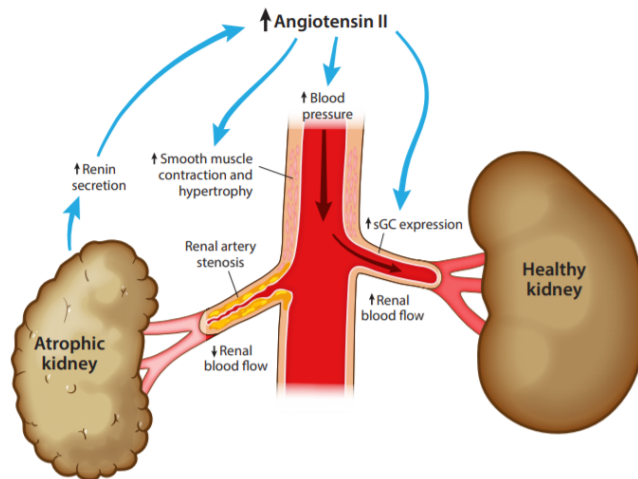
Joseph Galley¹, Scott Hahn¹, Megan Miller¹, Brittany Durgin¹, Edwin Jackson¹, Sean Stocker¹, and A Straub¹

¹University of Pittsburgh

September 11, 2020

Abstract

Background and Purpose: Reduced renal blood flow triggers activation of the renin-angiotensin-aldosterone system (RAAS) leading to renovascular hypertension. Renal vascular smooth muscle expression of the nitric oxide (NO) receptor, soluble guanylyl cyclase (sGC), modulates the vasodilatory response needed to control renal vascular tone and blood flow. Here, we tested if angiotensin II (Ang II) impacts sGC expression via an Ang II type 1 receptor (AT₁R)-forkhead box subclass O (FoxO) transcription factor dependent mechanism. **Experimental Approach:** Using a murine 2-kidney-1-clip (2K1C) renovascular hypertension model, we measured renal artery vasodilatory function and sGC expression. Additionally, we conducted cell culture studies using rat renal pre-glomerular smooth muscle cells (RPGSMCs) to test the in vitro mechanistic effects of Ang II treatment on sGC expression and downstream function. **Key Results:** Contralateral, unclipped renal arteries in 2K1C mice showed increased NO – dependent vasorelaxation compared to sham control mice. Immunofluorescence studies revealed increased sGC protein expression in contralateral unclipped renal arteries over sham controls. RPGSMCs treated with Ang II caused a significant upregulation of sGC mRNA and protein expression as well as downstream sGC-dependent signaling. Ang II signaling effects on sGC expression occurred through an AT₁R and FoxO transcription factor – dependent mechanism at both the mRNA and protein expression levels. **Conclusion and Implications:** Renal artery smooth muscle, in vivo and in vitro, upregulate expression of sGC following RAAS activity. In both cases, upregulation of sGC leads to elevated downstream cGMP signaling, suggesting a previously unrecognized protective mechanism to improve renal blood flow.



SUMMARY:

- What is already known: Renovascular hypertension is an underlying cause of secondary and resistant hypertension.
- What this study adds: Angiotensin II stimulation of renal vasculature elevates sGC expression via an AT_1R and FoxO-dependent mechanism.
- Clinical significance: Enhanced sGC-mediated cGMP signaling affords protection through decreased renovascular tone and increased renal blood flow.

INTRODUCTION:

Renovascular hypertensive patients constitute 24.2% of all patients with drug resistant hypertension (Benjamin, et al., 2014), a condition characterized by persistent Stage I hypertension despite treatment with three or more adequately dosed anti-hypertensive therapies (Carey, et al., 2019). While the prevalence in the general population is low (1-2%) (Derckx and Schalekamp, 1994), renovascular hypertension is more common in elderly patients over age 65 (6.8%) and is present in nearly 40% of individuals with established peripheral or coronary artery disease (Goldfarb, 2003), (Iglesias, et al., 2000). Approximately 90% of renovascular hypertension stems from atherosclerotic renal artery stenosis (ARAS) (Meurer et al., 2009), (Sawicki, et al., 1991), (Tollefson and Ernst, 1991). ARAS leads to obstruction of renal artery blood flow, resulting in renin-angiotensin-aldosterone-system (RAAS) activation and subsequent elevation of circulating blood plasma angiotensin II (Ang II) (Goldblatt, et al., 1934). In response, the non-stenosed renal artery is subjected to increased blood flow leading to augmented sodium and water excretion by the kidney. This process, known as pressure natriuresis, helps to mitigate increased fluid retention, volume overload, and systemic blood pressure (Selkurt, 1951).

A main contributor to pressure natriuresis is endothelial-derived nitric oxide (NO), which has been shown to play a critical role in the dilation of the renal vasculature (Dautzenberg, et al., 2011), (Majid and Navar 2001), (Majid, et al., 1998), (O'Connor and Cowley 2010). NO diffuses to vascular smooth muscle cells (VSMCs) where it binds its cognate receptor, soluble guanylyl cyclase (sGC), which produces cGMP to elicit vasorelaxation (Arnold, et al., 1977), (Kuo and Greengard 1970). Of clinical importance, sGC modulating compounds, which enhance cGMP production, are currently under investigation for treatment of renal and cardiovascular diseases (Stasch, et al., 2015). In addition, we have recently shown that basal sGC expression is regulated by the forkhead box subclass O (FoxO) transcription factors in aortic VSMCs (Galley, et al., 2019).

Based on this evidence, we hypothesized that renal artery smooth muscle responds to elevated RAAS signaling with amplified sGC-mediated production of cGMP. In this study, we used a two-kidney-one-clip (2K1C) hypertension model, wherein blood flow to one renal artery is reduced (Goldblatt, et al., 1934), as a model of RAAS activation and renal hypertension. We find that renal smooth muscle responds to increased levels of Ang II by increasing the expression of sGC. This increased sGC expression occurs in an Ang II type 1 receptor (AT₁R) and FoxO transcription factor-dependent manner. Downstream, this results in enhanced cGMP signaling and increased smooth muscle relaxation. These studies are first to show that exposure of renal smooth muscle to elevated Ang II results in a protective mechanism whereby sGC expression is increased and leads to elevated cGMP production and vasorelaxation.

METHODS:

2K1C Renal Stenosis Model:

Eight week old C57B6/J male mice (Jackson Laboratories) were anesthetized with 2-3% isoflurane in 100% O₂. Through a retroperitoneal incision, the right renal artery was carefully isolated from the renal nerve. A 0.5 mm polytetrafluoroethylene catheter (ID: 0.008 X OD: 0.014; Braintree Scientific, SUBL140) was cut longitudinally, placed around the right renal artery, distal to the adrenal artery, and secured with two 10-0 sutures. Right renal arteries were exposed with no clip placed for sham control procedures. Animals were treated by subcutaneous injection of 0.03 mg/kg buprenorphine twice/day for 48 hours (Henry Schein Inc.) and 2 mg/kg enrofloxacin (Norbrook Laboratories) as previously published (Ong, et al., 2019). Mice were fed a 0.1% NaCl diet as previously described (DeLalio, et al., 2020), and animals were sacrificed 19-21 days following renal clip or sham surgery.

Animal harvesting for immunohistochemical analysis:

Male C57BL6/J mice with or without renal stenosis were sacrificed via CO₂ asphyxiation followed by cervical dislocation. Contralateral (right) renal arteries were excised and placed in 4% paraformaldehyde in PBS for 24 hours then placed in 100% ethanol for processing. Tissues were embedded in paraffin and sectioned at 8 μm thickness. Immunohistochemical analysis was performed as previously described (Durgin, et al., 2019). Tissue sections were deparaffinized with xylenes and rehydrated by sequentially decreased concentrations of ethanol (100%-70%) followed by deionized distilled water. Heat-mediated antigen retrieval was then performed using citric acid-buffer (Vector Laboratories, H-3300) for 20 minutes, then sections cooled for 30 minutes at 4°C. Sections were then blocked in 10% horse serum (Sigma H1138) in PBS (MilliporeSigma, H1270) at room temperature for 1 hour. Primary antibodies (See Table 1) for sGCβ (Cayman Chemical, 160897, 1:100) and von Willebrand Factor (VWF; Abcam, ab11713, 1:250) were incubated on sections in PBS containing 10% horse serum overnight at 4°C in a humidity chamber. One section per slide was stained with rabbit (Vector Laboratories, I-1000) IgG control to match corresponding sGCβ antibody concentration. Tissue sections were washed thrice, 5 minutes each with PBS. Sections were then incubated in PBS containing 10% horse serum with smooth muscle α-actin (ACTA2) primary antibody pre-conjugated to FITC fluorophore (MilliporeSigma, F3777 clone 1A4, 1:500), 4',6-diamidino-2-phenylindole (DAPI, D3571, Thermo Fisher Scientific, 1:100) and secondary antibodies (See Table 1) donkey anti-rabbit AlexaFluor 594 (Invitrogen, A-21207, 1:250) and donkey anti-sheep AlexaFluor 647 (Invitrogen, A-21447, 1:250) for 1 hour at room temperature in a humidity chamber. Tissue sections were then washed thrice in PBS for 5 minutes before being mounted on coverslips using Prolong Gold Antifade mounting medium with DAPI reagent (Invitrogen, P36931). Immunohistochemistry staining of renal arteries were imaged using a Nikon A1 Confocal Laser Microscope at the University of Pittsburgh Center for Biological Imaging. Images were taken with 40X objective magnification with 1024 x 1024 pixel resolution. Increments for Z-stacks of 1 μm were applied for stained and IgG controls. In ImageJ, a region of interest was drawn around ACTA2+ areas representing the smooth muscle cell tunica media then superimposed on sGCβ images for quantification of medial smooth muscle sGCβ expression.

Treatment of Renal Artery Rings and Myography:

The following treatment method was performed as previously described (Durgin, et al., 2019). In brief, murine renal arteries were rapidly cleaned, excised, cut into 2 mm rings, and placed in room temperature physiological salt solution (PSS) which contains: 119 mM NaCl, 4.7 mM KCl, 1.17mM MgSO₄, 1.18 mM KH₂PO₄, 5.5 mM D-glucose, 25 mM NaHCO₃, 0.027 mM EDTA, and 2.5 mM CaCl₂. Rings were then placed on a small vessel wire myograph (DMT 620M) filled with PSS (pH 7.4 when bubbled with 95% O₂ 5% CO₂ at 37°). Following a 30 minute rest, arteries were then gradually stretched to a tension corresponding to a transmural pressure of 80 mmHg. Arteries were then constricted with a dose response of phenylephrine (50 nM - 50 mM). Rings were washed 3 times with PSS and allowed to rest for 30 minutes. A final wash was performed, and arteries were rested for an additional 10 minutes. Following the final 10 minute rest period, arteries were constricted with a single dose of phenylephrine (1 mM). After reaching a plateau, a continuous dose response curve to ACh (10 µM-10 mM, Sigma, MA6625) or sodium nitroprusside (SNP; 1 nM-10 mM, Sigma, 71778) was administered to assess endothelium-dependent and NO-dependent relaxation, respectively. Maximal dilatory responses were subsequently determined using 100 µM SNP in Ca²⁺-free PSS. The percentage relaxation reported represents the data normalized to the maximal dilation by 100 µM SNP in Ca²⁺-free PSS in phenylephrine-constricted vessels.

Cell culture, drug, and peptide treatments:

Renal pre-glomerular smooth muscle cells (RPGSMCs) were isolated from Wistar-Kyoto rats as previously described (Zhu and Jackson, 2017) and cultured at 37°C in SmGm-2 fully supplemented growth medium (Lonza, CC-3181) containing 0.5% FBS and SmGm-2 SingleQuot (Lonza, CC-3182) reagents and passaged using 1X trypsin-EDTA (Gibco, 10779413) dissolved in 1X PBS. During drug treatments, RPGSMCs were washed twice with 1X PBS and cultured in serum and growth factor starved Dulbecco's Modified Eagle Medium/Ham's F12 (DMEM/F12, Sigma, D6421) media containing: 100 U/mL penicillin/streptomycin (Gibco, 15140-122), 1.6 mM L-glutamine (Gibco, 25030-081), 200 µM L-ascorbic acid, 5 µg/mL apo-transferrin, and 6.25 ng/mL sodium-selenite. Losartan (Cayman Chemicals, 124750-99-8), PD123319 (Sigma, 136676-91-0), and AS18428456 FoxO inhibitor (Cayman, A15871) were dissolved in dimethyl sulfoxide (DMSO, D8418), while Angiotensin II (Ang II, Sigma, A9525) peptide was dissolved in sterile deionized distilled water for stock solutions prior to treatment. Treatment concentrations for Losartan, PD123319, AS1842856, and Ang II were 100 nM, 100 nM, 1 µM and 1 µM, respectively. Control treatments involved 0.1% DMSO treatment for 48 hours prior to harvesting. For NO stimulation experiments, cells were pretreated with 10 µM sildenafil citrate (Sigma, PZ0003) for 45 minutes to inhibit cGMP-specific phosphodiesterase 5 activity, and then stimulated with the NO-donor, diethylammonium (Z)-1-(N,N-diethylamino)diazen-1-ium-1,2-diolate (DEA-NONOate, Cayman, 82100), for 15 minutes prior to lysis.

qRT-PCR:

RPGSMCs were grown in 6-well plates until approximately 90% confluent before being washed and switched to serum and growth factor starved media. Cells were then subjected to 48-hour drug and/or peptide treatment before lysis in TRIzol reagent (ThermoFisher, 15596026). The Direct-zol RNA miniprep plus (Zymo, R2051) manufacturer's protocol was used to isolate RNA from cells. For cDNA synthesis, the SuperScript IV First Strand Synthesis (ThermoFisher, 18091050) kit manufacturer's protocol was used. For quantitative real time PCR analysis, the PowerUp SyBr Green (ThermoFisher, A25742) and 1 µM target primer (Table 2) were mixed according to manufacturer's protocol with settings for 40 PCR cycles, 95°C melting temperature, 58°C annealing temperature, and 72°C extension temperature set on a QuantStudio 5 Real-Time 384-well PCR System (ThermoFisher A28140) for amplification. The $\Delta\text{-}\Delta\text{-ct}$ value fold change in expression was used in order to control for cell number and RNA quality with values normalized to an 18S housekeeping gene transcript.

Western blot:

RPGSMCs were cultured in 12-well culture dishes until approximately 90% confluent before being switched to serum and growth factor starved media for 48 hours. Cells were then washed with PBS and 1X Cell Lysis Buffer (Cell Signaling, 9803) containing: (pH 7.5) 20 mM Tris-HCl, 1 mM Na₂EDTA, 1 mM EGTA,

1% Triton, 1 mM β -glycerophosphate, 1 mM Na_3VO_4 , 1 $\mu\text{g}/\text{mL}$ leupeptin, 2.5 mM sodium pyrophosphate, and additional 1X protease (MilliporeSigma P8340) and phosphatase inhibitors (MilliporeSigma, P5726) at 4°C. A bicinchoninic acid kit (ThermoFisher, 23225) was used to quantify lysate protein concentration and approximately 15 μg of protein was used for each western blot lane. Lysates were boiled at 100°C for 10 minutes and Laemmli buffer was added such that final lysates contained: (pH 6.8) 31.5 mM Tris-HCl, 10% glycerol, 1% SDS, 2.5% β -mercaptoethanol and 0.005% Bromophenol Blue before being loaded onto 4-12% gradient BisTris polyacrylamide gels (Invitrogen Life Technologies, NP0335BOX). Proteins were transferred from polyacrylamide gels to nitrocellulose membranes (LiCor, 926-31092) and blocked for approximately 30 minutes at room temperature with 1% BSA in PBS. Membranes were incubated in primary antibody (Table 1) solution containing 1% BSA in PBST overnight at 4°C. An Odyssey CLx Imager (LiCor, 9140) was used for fluorescence visualization and semi-quantitative analysis was performed using Image Studio software.

Immunocytochemical analysis of hypertrophy:

RPGSMCs were cultured on a single 24x50 mm cover glass (VWR, 16004-322) to approximately 90% confluency and then serum starved in DMEM/F12 for 48 hours. Media was then gently aspirated by hand and the cover glass washed with PBS containing 0.1% Triton X-100 for 5 minutes. Cells were then fixed in 4% paraformaldehyde in PBS for 30 minutes at room temperature and then gently washed twice with PBS containing 0.1% Triton X-100. RPGSMCs blocking was carried out in PBS with 10% horse serum for 1 hour at room temperature. Primary antibody incubation for rabbit-sGC β and sheep-vWF (See Table 1) incubation was carried out in PBS with 10% horse serum overnight at 4°C in a humidified chamber. Cells were then gently washed thrice with PBS for 5 min each time before being incubated in either primary ACTA2 antibody conjugated to FITC fluorophore or AlexaFluor donkey anti-rabbit secondary antibody (See Table 1) for 1 hour at room temperature in PBS containing 10% horse serum. Cells were gently washed twice for 5 min in PBS before applying Prolong Gold Antifade mounting medium with DAPI reagent (Invitrogen, P36931). Immunocytochemistry images of RPGSMCs were taken using a Leica DM1000 microscope at 40x objective with 2X zoom applied and cell area was quantified using ImageJ software.

Statistics:

Statistical analyses were performed using Graphpad Prism Software 7.0d. For wire myography, p-values represent significance by two-way ANOVA analysis with Sidak multiple comparisons tests for comparisons between groups at each vasodilator concentration. Based upon normality using a Shapiro-Wilk test, p-values for statistics in qPCR, Western blot, and immunostaining were assessed using either an unpaired two-tailed t -test or unpaired two-tailed t -test with Welch's correction. Symbols were consistent throughout wherein * denotes $p < 0.05$, ** denotes $p < 0.01$, *** denotes $p < 0.001$, and **** $p < 0.0001$.

RESULTS:

To determine the effects of RAAS activation on the renal vasculature, we used a two-kidney-one-clip (2K1C) model (Figure 1A), which involves surgical stenosis of one of the renal arteries. To assess the vasoreactivity responses of the unclipped contralateral (right) renal arteries, wire myography was performed on the right (unclipped) renal arteries of clipped and sham control animals. We observed that contralateral clipped arteries contracted significantly less to 10 μM phenylephrine than their sham counterparts (Figure 1B). We also observed a significant improvement in endothelium-dependent vasodilation in response to ACh (Figure 1C). The calculated values with respect to sham control and renal clip animals is $1.6 \times 10^{-7} \text{M} \pm 4.0 \times 10^{-8} \text{M}$ and $1.1 \times 10^{-7} \text{M} \pm 3.2 \times 10^{-8} \text{M}$, respectively for EC_{50} , and we observed $55.9 \pm 5.2\%$ and $76.8 \pm 5.1\%$, respectively for E_{max} values. Similarly, a significant improvement in NO-dependent vasodilation in response to the NO-donor, sodium nitroprusside (SNP), was observed (Figure 1D) with calculated EC_{50} values of $3.99 \times 10^{-5} \text{M} \pm 3.95 \times 10^{-5} \text{M}$ and $1.22 \times 10^{-5} \text{M} \pm 7.83 \times 10^{-6} \text{M}$ for sham and renal clip groups, respectively. These data also show a calculated E_{max} of $44.5 \pm 4.5\%$ versus $66.3 \pm 4.2\%$ for sham control and clipped animals, respectively. These findings indicate a significant improvement in the vasorelaxation responses of the contralateral clipped arteries over sham controls to both an endothelium-dependent vasodilator and a NO-donor.

To determine if the increased NO-dependent vasodilatory response in contralateral clipped arteries were due

to changes in sGC expression, we quantified protein expression within renal arteries. We found that the expression of the β subunit of sGC (sGC β) was significantly elevated in contralateral renal arteries of clipped animals (Figure 2B, F) compared to sham controls. No significant differences were seen in nuclei staining (Figure 2A, E), smooth muscle α -actin (ACTA2) expression (Figure 2C, G), or the endothelial cell marker, von Willebrand Factor (vWF, Figure 2D, H), between groups.

Next, we sought to determine what drives sGC expression changes in renal artery smooth muscle. It is well established that reduced renal blood flow increases angiotensin II (Ang II) in models of 2K1C (Murphy, et al., 1984), (Sadjadi, et al., 2002). Therefore, we treated rat renal preglomerular smooth muscle cells (RPGSMCs) with vehicle or 10^{-6} M Ang II to test if Ang II increased sGC expression. Ang II treatment led to increased RPGSMC cell area and augmented filamentous (F)-actin expression (Figure 3B, E), indicating RPGSMC hypertrophy (Stephenson, et al., 1998). Additionally, Ang-II resulted in increased sGC β protein expression by 1.7-fold via immunofluorescence and 4-fold via western blot analysis (Figure 3C, F, G). Consistent with increased sGC protein expression, we found that Ang II treatment also caused a 3.6-fold increase in sGC α mRNA (Figure 4A) and a 4.4-fold increase in sGC β mRNA (Figure 4B). To test if increased sGC expression impacted cGMP production and PKG activity, RPGSMCs treated with Ang II or vehicle, and subjected to treatment with the NO donor, DEA-NONOate, for 15 minutes prior to harvest to induce sGC-mediated cGMP production. Quantification of vasodilator stimulated protein (VASP) phosphorylated at the serine 239 position, a surrogate indicator of cGMP-dependent protein kinase activity (Smolenski, et al., 1998), showed an 8-fold increase in pVASP in Ang II-treated cells stimulated with DEA-NONOate compared to vehicle controls (Figure 3H). Taken together, these data show that Ang II *in vitro* augments sGC expression and cGMP signaling, indicating that elevated RAAS activity increases sGC expression and downstream signaling *in vivo*.

We next tested which Ang II receptor subtype- either the AT₁R or the Angiotensin Type 2 Receptor (AT₂R) -was responsible for increasing sGC mRNA and protein expression. RPGSMCs co-treated Ang II and Losartan, an AT₁R antagonist (Timmermans, et al., 1995), caused inhibition of Ang II – induced increases in sGC α mRNA (Figure 4A), sGC β mRNA (Figure 4B), and sGC β protein expression (Figure 4C & D). Conversely, RPGSMCs co-treated with Ang II and PD123319, an AT₂R antagonist (Blankley, et al., 1991), showed no significant impact on the Ang II – induced increases in sGC α mRNA (Figure 4A), sGC β mRNA (Figure 4B), or sGC β protein expression (Figure 4C & D).

Recently, we published evidence that the FoxO family of transcription factors regulate the mRNA expression of sGC in aortic smooth muscle (Galley, et al., 2019). To determine whether the FoxO family of transcription factors also influence the function of renal smooth muscle, we treated RPGSMCs with 10^{-6} M AS1842856, a small molecule Fox O transcription factor inhibitor (Nagashima, et al., 2010), alone and in conjunction with Ang II. When AS1842856 was administered alone to RPGSMCs, a significant reduction in sGC α mRNA (Figure 5A), sGC β mRNA (Figure 5B), and sGC β protein expression (Figure 5C) was observed. When administered with Ang II, AS1842856 produced no effect on either sGC α mRNA (Figure 5A), sGC β mRNA (Figure 5B), or sGC β protein expression (Figure 5C) when compared to vehicle controls. These data indicate the FoxO transcription factors are necessary for the Ang II-mediated sGC expression increases in renal smooth muscle.

Next, we tested Ang II receptor antagonists and FoxO inhibitors on cGMP production, determined by pVASP expression following NO-stimulation with DEA-NONOate. At baseline, where no DEA-NONOate-stimulation occurred, no significant differences were observed between the treatment groups. Similar to the observed effect in sGC expression, co-treatment with Ang II and PD123319 produced significant increases in downstream sGC function via VASP phosphorylation following DEA-NONOate stimulation compared to controls treated with DEA-NONOate. AS1842856 or Losartan showed no significant differences from control-treated cells stimulated with DEA-NONOate (Figure 6A & B). These data show that PD123319 has no significant effect and that the blunting effect of Losartan or AS1842856 on the Ang II-mediated responses also inhibited downstream cGMP signaling following NO-dependent stimulation.

DISCUSSION:

Renal artery stenosis remains a pervasive cause of secondary hypertension and a condition significantly correlated with high morbidity and mortality (Textor, 2003), (Kalra, et al., 2005), (de Mast and Beutler, 2009), (Kalra, et al., 2010). NO plays an important role in maintaining renal blood flow and glomerular filtration rate following single renal artery stenosis (Granger, et al., 2002), (Majid and Navar, 1997), (Majid, et al., 1998). In addition, there is emerging pre-clinical evidence that sGC stimulator drugs which have had notable anti-fibrotic effects, in conjunction with RAAS blockade confer resistance to end stage renal disease and chronic kidney disease, (Beyer, et al., 2015), (Sandner and Stasch, 2017). Such therapies have demonstrated an ability to elevate blood flow and/or improve cardiac outcomes as a result of decreased vascular tone and decreased blood pressure (Stasch, et al., 2001), (Stasch, et al., 2011), (Evgenov, et al., 2006). Our previous study, in accordance with previous 2K1C models, showed that the modified 2K1C renal artery stenosis model causes increased blood pressure without altering body weight or plasma salt concentrations (DeLalio, et al., 2020). Here we provide the first evidence that sGC expression unexpectedly increases in renal artery vascular smooth muscle to preserve renal blood flow.

In this study, we observed a significant increase in vasodilation in the contralateral renal arteries of renal clipped animals, which was not observed in other arterial beds. This increase in vasodilation was likely due to the measurable increase in sGC expression observed in unobstructed renal artery smooth muscle from clipped animals compared to their sham controls. We also observed a significant increase in ACh-dependent vasodilation of renal clip animals over the sham controls, suggesting significant contribution of the endothelium in this response. This response may indicate that NO signaling, in the endothelium, which has been established to be a pivotal player in promoting regulation of renovascular homeostasis of blood pressure and fluid retention (O'Connor and Cowley, 2010), (Dautzenberg, et al., 2011), is enhanced compared with other vascular beds following elevated RAAS activity.

Changes in sGC expression in renal smooth muscle were not limited to *in vivo* animal tissue chronically exposed to Ang II. Following treatment of cultured renal pre-glomerular smooth muscle cells (RPGSMCs) with Ang II for 48 hours, the increase observed in sGC mRNA and protein expression suggests that RPGSMCs respond differently from aortic smooth muscle. Aortic smooth muscle and endothelial cells exhibit decreased functional NO signaling with excess Ang II exposure, via pathological overproduction of reactive oxygen species (ROS) (Griendling, et al., 1994), (Doughan, et al., 2008). Moreover, aortic sGC protein expression decreases with Ang II (Mollnau, et al., 2002), (Rippe, et al., 2017), and Ang II impairs aortic smooth muscle sGC function (Rippe, et al., 2017), (Crassous, et al., 2012). Furthermore, these processes prevent sufficient cGMP production, leading to elevated systemic blood pressure (Durgin, et al., 2019). On the contrary, our studies show that treatment with Ang II in conjunction with NO-stimulation caused elevated cGMP signaling in RPGSMCs, as indicated by VASP phosphorylation. This indicates enhanced sGC-cGMP signaling following Ang II treatment in renal vascular smooth muscle.

Remarkably, other known responses to Ang II treatment were noted in RPGSMCs, such as increased protein expression, elevated F-actin expression, and increased cell size. These patterns have been observed in aortic smooth muscle both *in vivo* following infusion with Ang II and *in vitro* following Ang II treatment in culture, (Geisterfer, et al., 1988), (Zhang, et al., 2005). This suggests that while the increases in sGC expression are unique to renal smooth muscle, the hypertrophic responses to Ang II conform to the patterns that have been observed by others.

Specifically, our data shows that the AT₁R, but not the AT₂R, is responsible for the elevated expression of sGC observed in renal smooth muscle in response to Ang II. Indeed, co-treatment with Losartan and Ang II was sufficient to reverse all of the Ang II-induced phenotypes we observed in RPGSMCs, while Ang II co-treatment with PD123319 did not impact any of the phenotypes facilitated by Ang II treatment alone. This response may be due to the high density of AT₁Rs that have been observed in the adventitia of the renal vasculature (Doughan, et al., 2008), (Harrison-Bernard, et al., 1997), and the increased constriction of renal vasculature and, to a smaller extent, gut vasculature following acute Ang II infusion (Jackson and Herzer, 2001). Curiously, this contrasts with the role for the AT₂R in cardiac function, which has been shown to improve outcomes following treatment with AT₂R-specific agonists following myocardial infarction

(Kaschina, et al., 2008). These findings suggest that the observed effect on sGC expression and function are largely independent of AT₂R activation. Truncation products such as angiotensin 1-7 or angiotensin IV may also play a role (Savergnini, et al., 2010), (Esteban, et al., 2005), albeit minor. Taken together, these findings suggest that renal smooth muscle responds uniquely to Ang II via the AT₁R to promote increased sGC expression and sGC-cGMP induced vasodilation while maintaining the canonical hypertrophic responses associated with elevated Ang II exposure.

Consistent with our previous work in aortic SMCs (Galley, et al., 2019), Ang II studies in RPGSMCs showed that inhibition of the forkhead box subclass O (FoxO) transcription factors significantly impairs sGC expression. This finding indicates FoxO regulation of sGC expression applies to multiple vascular beds, thus regulating dilatory function in multiple branches of the vascular tree. The FoxO protein(s) responsible are not yet known and the specific role of the FoxO transcription factors in the development and pathology of renal artery stenosis requires further study to assess their diverse functions in vascular physiology. It is nevertheless clear that the Ang II-mediated increases in sGC function cannot occur without functional FoxO transcription factor activity. Ang II can activate Akt (Li and Malik, 2005), and Akt-mediated phosphorylation is a common regulatory mechanism known to modulate FoxO transcriptional activity (Biggs, et al., 1999), (Brunet, at al., 1999), (Kops, et al., 1999). In addition, Ang II has been shown to cause increases in ROS, and oxidative stress is known to impact FoxO transcription factor activity through acetylation/deacetylation (Salminen, et al., 2013), (Ichiki, et al., 2003), (Motta, et al., 2004), (van der Horst, et al., 2004). These findings suggest that there could be an indirect regulatory mechanism between the AT₁R and FoxO transcription factors. Future research in this area should investigate the potential mechanistic links between agonism of the AT₁R and activation of the FoxO transcription factors. Moreover, our research has shown that oxidation or loss of sGC heme iron leads to NO insensitivity, making the protein more responsive to sGC activating compounds which target oxidized or heme-deficient sGC to produce cGMP (Rahaman, et al., 2017), (Durgin, et al., 2019). Investigation of Ang II-mediated ROS production may reveal a novel therapeutic target for sGC activating drugs under conditions where high RAAS activity promotes oxidative stress.

Collectively, we show for the first time that in response to elevated RAAS activity, renal smooth muscle responds through an AT₁R and FoxO transcription factor-dependent mechanism to increase sGC expression and cGMP signaling. These responses likely constitute a compensatory response to allow for maintenance of homeostatic blood volume and salt balance to counteract Ang II-dependent increases in systemic blood pressure, and a means of preserving normal body weight and plasma sodium concentration. Combined, this study marks an important discovery of how the renal vasculature responds to elevated circulating plasma Ang II, advancing our understanding of renal vascular hypertension and the regulation of cGMP signaling within the renal vascular wall.

ACKNOWLEDGEMENTS:

We would like to acknowledge the Center for Biological Imaging at the University of Pittsburgh for its support and confocal microscope usage and Dr. Delphine Gomez for use of her microscope at the University of Pittsburgh. Financial support for this work was provided by the National Institutes of Health (NIH) [grants R01 HL 133864 and R01 HL 128304], American Heart Association (AHA) Grant-in-Aid [16GRNT27250146] (A.C.S.), NIH F31 Pre-Doctoral Fellowship Award [HL 151173], Louis J. Ignarro Cardiovascular Fellowship [5T32GM008424], NIH T32 Division of Geriatrics Aging Institute Fellowship [AG021885] (J.C.G.), NIH T32 Post-Doctoral Fellowship Award [DK007052] (B.G.D.), NIH [grants DK091190, HL109002, HL069846, DK079307 (E.K.J.), and NIH [grant R01 HL152680 (S.D.S.)]. We would also like to acknowledge the support of Dr. Katherine C. Wood for her help editing and reviewing the manuscript for publication.

AUTHOR CONTRIBUTIONS:

Participated in research design: Galley, Durgin, Miller, Hahn, Stocker, Straub. Conducted experiments: Galley, Miller, Durgin, Hahn, Stocker. Contributed new reagents or analytic tools: Galley, Hahn, Durgin, Jackson, Stocker. Performed data analysis: Galley, Miller, Hahn. Wrote or contributed to the writing of the manuscript: Galley, Durgin, Straub.

REFERENCES :

- Arnold WP, Mittal CK, Katsuki S, & Murad F (1977). Nitric oxide activates guanylate cyclase and increases guanosine 3':5'-cyclic monophosphate levels in various tissue preparations. *Proc Natl Acad Sci U S A* 74: 3203-3207.
- Benjamin MM, Fazel P, Filardo G, Choi JW, & Stoler RC (2014). Prevalence of and risk factors of renal artery stenosis in patients with resistant hypertension. *Am J Cardiol* 113: 687-690.
- Beyer C, Zenzmaier C, Palumbo-Zerr K, Mancuso R, Distler A, Dees C, *et al.* (2015). Stimulation of the soluble guanylate cyclase (sGC) inhibits fibrosis by blocking non-canonical TGFbeta signalling. *Ann Rheum Dis* 74: 1408-1416.
- Biggs WH, 3rd, Meisenhelder J, Hunter T, Cavenee WK, & Arden KC (1999). Protein kinase B/Akt-mediated phosphorylation promotes nuclear exclusion of the winged helix transcription factor FKHR1. *Proc Natl Acad Sci U S A* 96: 7421-7426.
- Blankley CJ, Hodges JC, Klutchko SR, Himmelsbach RJ, Chucholowski A, Connolly CJ, *et al.* (1991). Synthesis and structure-activity relationships of a novel series of non-peptide angiotensin II receptor binding inhibitors specific for the AT2 subtype. *J Med Chem* 34:3248-3260.
- Brunet A, Bonni A, Zigmond MJ, Lin MZ, Juo P, Hu LS, *et al.*(1999). Akt promotes cell survival by phosphorylating and inhibiting a Forkhead transcription factor. *Cell* 96: 857-868.
- Carey RM, Sakhuja S, Calhoun DA, Whelton PK, & Muntner P (2019). Prevalence of Apparent Treatment-Resistant Hypertension in the United States. *Hypertension* 73: 424-431.
- Crassous PA, Couloubaly S, Huang C, Zhou Z, Baskaran P, Kim DD, *et al.* (2012). Soluble guanylyl cyclase is a target of angiotensin II-induced nitrosative stress in a hypertensive rat model. *Am J Physiol Heart Circ Physiol* 303: H597-604.
- Dautzenberg M, Keilhoff G, & Just A (2011). Modulation of the myogenic response in renal blood flow autoregulation by NO depends on endothelial nitric oxide synthase (eNOS), but not neuronal or inducible NOS. *J Physiol* 589: 4731-4744.
- de Mast Q, & Beutler JJ (2009). The prevalence of atherosclerotic renal artery stenosis in risk groups: a systematic literature review. *J Hypertens* 27: 1333-1340.
- DeLalio LJ, Hahn S, Katayama PL, Wenner MM, Farquhar WB, Straub AC, *et al.* (2020). Excessive dietary salt promotes aortic stiffness in murine renovascular hypertension. *Am J Physiol Heart Circ Physiol* 318: H1346-H1355.
- Derckx FH, & Schalekamp MA (1994). Renal artery stenosis and hypertension. *Lancet* 344: 237-239.
- Doughan AK, Harrison DG, & Dikalov SI (2008). Molecular mechanisms of angiotensin II-mediated mitochondrial dysfunction: linking mitochondrial oxidative damage and vascular endothelial dysfunction. *Circ Res* 102: 488-496.
- Durgin BG, Hahn SA, Schmidt HM, Miller MP, Hafeez N, Mathar I, *et al.* (2019). Loss of smooth muscle CYB5R3 amplifies angiotensin II-induced hypertension by increasing sGC heme oxidation. *JCI Insight* 4.
- Esteban V, Ruperez M, Sanchez-Lopez E, Rodriguez-Vita J, Lorenzo O, Demaegdt H, *et al.* (2005). Angiotensin IV activates the nuclear transcription factor-kappaB and related proinflammatory genes in vascular smooth muscle cells. *Circ Res* 96: 965-973.
- Evgenov OV, Pacher P, Schmidt PM, Hasko G, Schmidt HH, & Stasch JP (2006). NO-independent stimulators and activators of soluble guanylate cyclase: discovery and therapeutic potential. *Nat Rev Drug Discov* 5: 755-768.

- Galley JC, Durgin BG, Miller MP, Hahn SA, Yuan S, Wood KC, *et al.*(2019). Antagonism of Forkhead Box Subclass O Transcription Factors Elicits Loss of Soluble Guanylyl Cyclase Expression. *Mol Pharmacol* 95: 629-637.
- Geisterfer AA, Peach MJ, & Owens GK (1988). Angiotensin II induces hypertrophy, not hyperplasia, of cultured rat aortic smooth muscle cells. *Circ Res* 62: 749-756.
- Goldblatt H, Lynch J, Hanzal RF, & Summerville WW (1934). Studies on Experimental Hypertension : I. The Production of Persistent Elevation of Systolic Blood Pressure by Means of Renal Ischemia. *J Exp Med* 59: 347-379.
- Goldfarb DA (2003). Prevalence of renovascular disease in the elderly: a population-based study. *J Urol* 170: 1053-1054.
- Granger JP, Alexander BT, & Llinas M (2002). Mechanisms of pressure natriuresis. *Curr Hypertens Rep* 4: 152-159.
- Griendling KK, Minieri CA, Ollerenshaw JD, & Alexander RW (1994). Angiotensin II stimulates NADH and NADPH oxidase activity in cultured vascular smooth muscle cells. *Circ Res* 74: 1141-1148.
- Harrison-Bernard LM, Navar LG, Ho MM, Vinson GP, & el-Dahr SS (1997). Immunohistochemical localization of ANG II AT1 receptor in adult rat kidney using a monoclonal antibody. *Am J Physiol* 273: F170-177.
- Ichiki T, Tokunou T, Fukuyama K, Iino N, Masuda S, & Takeshita A (2003). Cyclic AMP response element-binding protein mediates reactive oxygen species-induced c-fos expression. *Hypertension* 42:177-183.
- Iglesias JI, Hamburger RJ, Feldman L, & Kaufman JS (2000). The natural history of incidental renal artery stenosis in patients with aortoiliac vascular disease. *Am J Med* 109: 642-647.
- Jackson EK, & Herzer WA (2001). Regional vascular selectivity of angiotensin II. *J Pharmacol Exp Ther* 297: 736-745.
- Kalra PA, Guo H, Gilbertson DT, Liu J, Chen SC, Ishani A, *et al.*(2010). Atherosclerotic renovascular disease in the United States. *Kidney Int* 77: 37-43.
- Kalra PA, Guo H, Kausz AT, Gilbertson DT, Liu J, Chen SC, *et al.*(2005). Atherosclerotic renovascular disease in United States patients aged 67 years or older: risk factors, revascularization, and prognosis. *Kidney Int* 68: 293-301.
- Kaschina E, Grzesiak A, Li J, Foryst-Ludwig A, Timm M, Rompe F, *et al.* (2008). Angiotensin II type 2 receptor stimulation: a novel option of therapeutic interference with the renin-angiotensin system in myocardial infarction? *Circulation* 118: 2523-2532.
- Kops GJ, de Ruiter ND, De Vries-Smits AM, Powell DR, Bos JL, & Burgering BM (1999). Direct control of the Forkhead transcription factor AFX by protein kinase B. *Nature* 398: 630-634.
- Kuo JF, & Greengard P (1970). Cyclic nucleotide-dependent protein kinases. VI. Isolation and partial purification of a protein kinase activated by guanosine 3',5'-monophosphate. *J Biol Chem* 245:2493-2498.
- Li F, & Malik KU (2005). Angiotensin II-induced Akt activation through the epidermal growth factor receptor in vascular smooth muscle cells is mediated by phospholipid metabolites derived by activation of phospholipase D. *J Pharmacol Exp Ther* 312: 1043-1054.
- Majid DS, & Navar LG (1997). Nitric oxide in the mediation of pressure natriuresis. *Clin Exp Pharmacol Physiol* 24: 595-599.
- Majid DS, & Navar LG (2001). Nitric oxide in the control of renal hemodynamics and excretory function. *Am J Hypertens* 14:74S-82S.

- Majid DS, Omoro SA, Chin SY, & Navar LG (1998). Intrarenal nitric oxide activity and pressure natriuresis in anesthetized dogs. *Hypertension* 32: 266-272.
- Mollnau H, Wendt M, Szocs K, Lassegue B, Schulz E, Oelze M, *et al.* (2002). Effects of angiotensin II infusion on the expression and function of NAD(P)H oxidase and components of nitric oxide/cGMP signaling. *Circ Res* 90: E58-65.
- Motta MC, Divecha N, Lemieux M, Kamel C, Chen D, Gu W, *et al.*(2004). Mammalian SIRT1 represses forkhead transcription factors. *Cell* 116: 551-563.
- Murphy WR, Coleman TG, Smith TL, & Stanek KA (1984). Effects of graded renal artery constriction on blood pressure, renal artery pressure, and plasma renin activity in Goldblatt hypertension. *Hypertension* 6: 68-74.
- Nagashima T, Shigematsu N, Maruki R, Urano Y, Tanaka H, Shimaya A, *et al.* (2010). Discovery of novel forkhead box O1 inhibitors for treating type 2 diabetes: improvement of fasting glycemia in diabetic db/db mice. *Mol Pharmacol* 78: 961-970.
- Ong J, Kinsman BJ, Sved AF, Rush BM, Tan RJ, Carratino MD, Stocker SD (2019). Renal sensory nerves increase sympathetic nerve activity and blood pressure in 2-kidney 1-clip hypertensive mice. *J Neurophysiol* 122(1): 358-367.
- O'Connor PM, & Cowley AW, Jr. (2010). Modulation of pressure-natriuresis by renal medullary reactive oxygen species and nitric oxide. *Curr Hypertens Rep* 12: 86-92.
- Rahaman MM, Nguyen AT, Miller MP, Hahn SA, Sparacino-Watkins C, Jobbagy S, *et al.* (2017). Cytochrome b5 Reductase 3 Modulates Soluble Guanylate Cyclase Redox State and cGMP Signaling. *Circ Res* 121:137-148.
- Rippe C, Zhu B, Krawczyk KK, Bavel EV, Albinsson S, Sjolund J, *et al.* (2017). Hypertension reduces soluble guanylyl cyclase expression in the mouse aorta via the Notch signaling pathway. *Sci Rep* 7:1334.
- Sadjadi J, Puttaparthi K, Welborn MB, 3rd, Rogers TE, Moe O, Clagett GP, *et al.* (2002). Upregulation of autocrine-paracrine renin-angiotensin systems in chronic renovascular hypertension. *J Vasc Surg* 36: 386-392.
- Salminen A, Kaarniranta K, & Kauppinen A (2013). Crosstalk between Oxidative Stress and SIRT1: Impact on the Aging Process. *Int J Mol Sci* 14: 3834-3859.
- Sandner P, & Stasch JP (2017). Anti-fibrotic effects of soluble guanylate cyclase stimulators and activators: A review of the preclinical evidence. *Respir Med* 122 Suppl 1: S1-S9.
- Savergnini SQ, Beiman M, Lautner RQ, de Paula-Carvalho V, Allahdadi K, Pessoa DC, *et al.* (2010). Vascular relaxation, antihypertensive effect, and cardioprotection of a novel peptide agonist of the MAS receptor. *Hypertension* 56: 112-120.
- Sawicki PT, Kaiser S, Heinemann L, Frenzel H, & Berger M (1991). Prevalence of renal artery stenosis in diabetes mellitus—an autopsy study. *J Intern Med* 229: 489-492.
- Selkurt EE (1951). Effect of pulse pressure and mean arterial pressure modification on renal hemodynamics and electrolyte and water excretion. *Circulation* 4: 541-551.
- Smolenski A, Bachmann C, Reinhard K, Honig-Liedl P, Jarchau T, Hoschuetzky H, *et al.* (1998). Analysis and regulation of vasodilator-stimulated phosphoprotein serine 239 phosphorylation in vitro and in intact cells using a phosphospecific monoclonal antibody. *J Biol Chem* 273: 20029-20035.
- Stasch JP, Becker EM, Alonso-Alija C, Apeler H, Dembowski K, Feurer A, *et al.* (2001). NO-independent regulatory site on soluble guanylate cyclase. *Nature* 410: 212-215.
- Stasch JP, Pacher P, & Evgenov OV (2011). Soluble guanylate cyclase as an emerging therapeutic target in cardiopulmonary disease. *Circulation* 123: 2263-2273.

Stasch JP, Schlossmann J, & Hocher B (2015). Renal effects of soluble guanylate cyclase stimulators and activators: a review of the preclinical evidence. *Curr Opin Pharmacol* 21: 95-104.

Stephenson LA, Haney LB, Hussaini IM, Karns LR, & Glass WF, 2nd (1998). Regulation of smooth muscle alpha-actin expression and hypertrophy in cultured mesangial cells. *Kidney Int* 54: 1175-1187.

Textor SC (2003). Managing renal arterial disease and hypertension. *Curr Opin Cardiol* 18: 260-267.

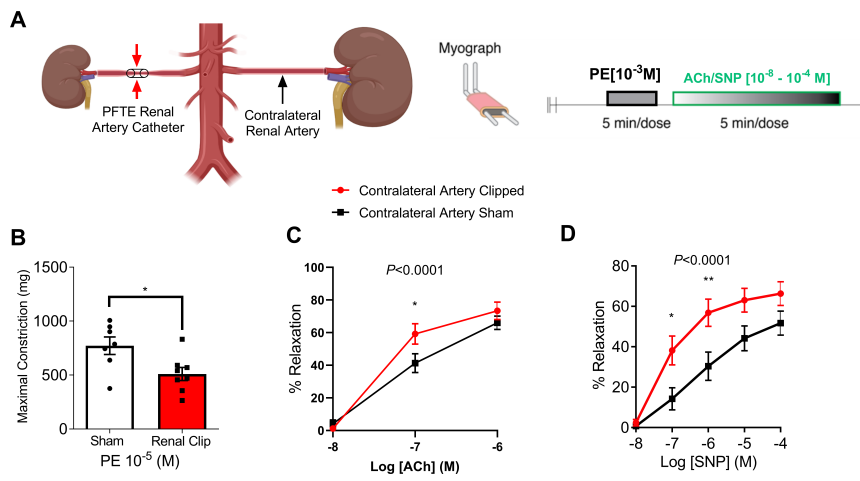
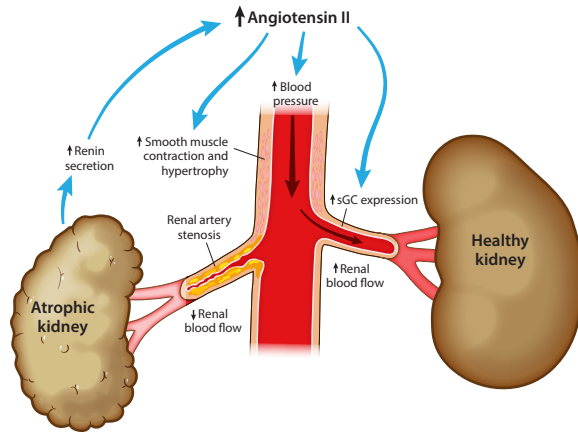
Timmermans PB, Duncia JV, Carini DJ, Chiu AT, Wong PC, Wexler RR, *et al.* (1995). Discovery of losartan, the first angiotensin II receptor antagonist. *J Hum Hypertens* 9 Suppl 5: S3-18.

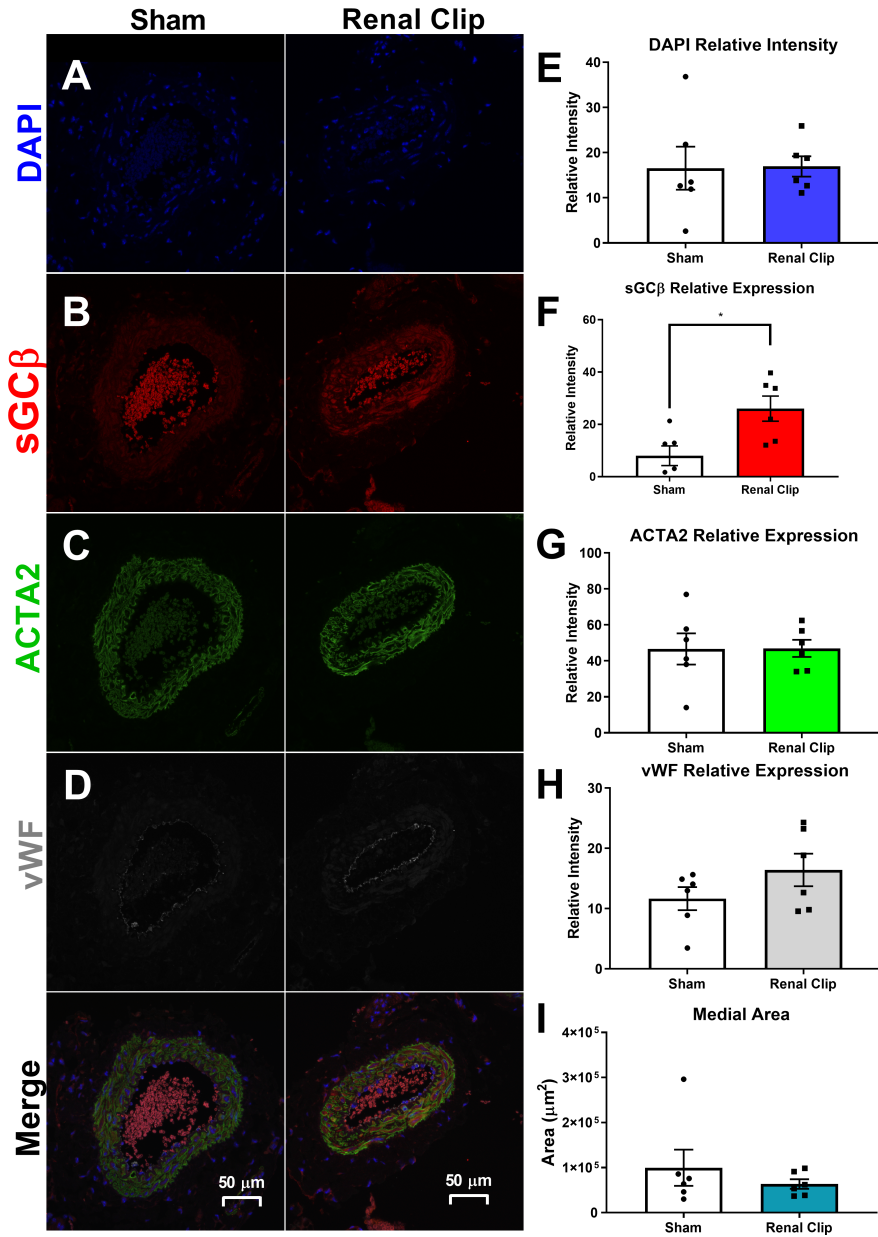
Tollefson DF, & Ernst CB (1991). Natural history of atherosclerotic renal artery stenosis associated with aortic disease. *J Vasc Surg* 14: 327-331.

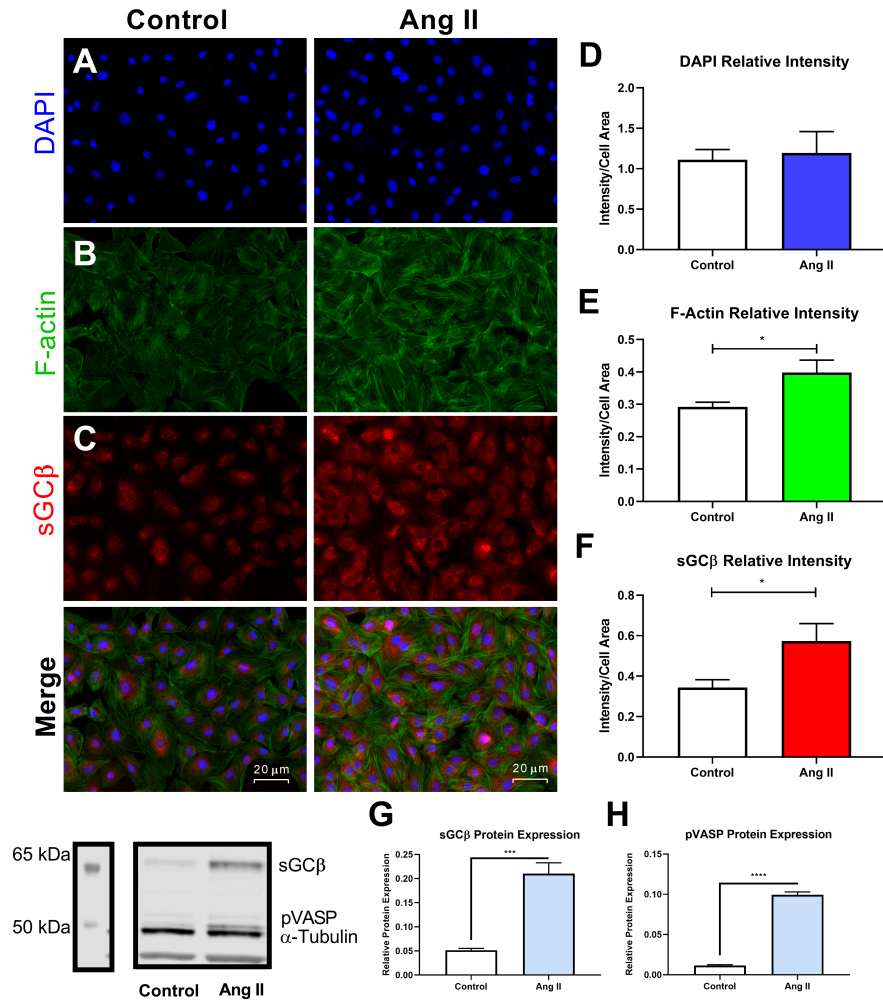
van der Horst A, Tertoolen LG, de Vries-Smits LM, Frye RA, Medema RH, & Burgering BM (2004). FOXO4 is acetylated upon peroxide stress and deacetylated by the longevity protein hSir2(SIRT1). *J Biol Chem* 279: 28873-28879.

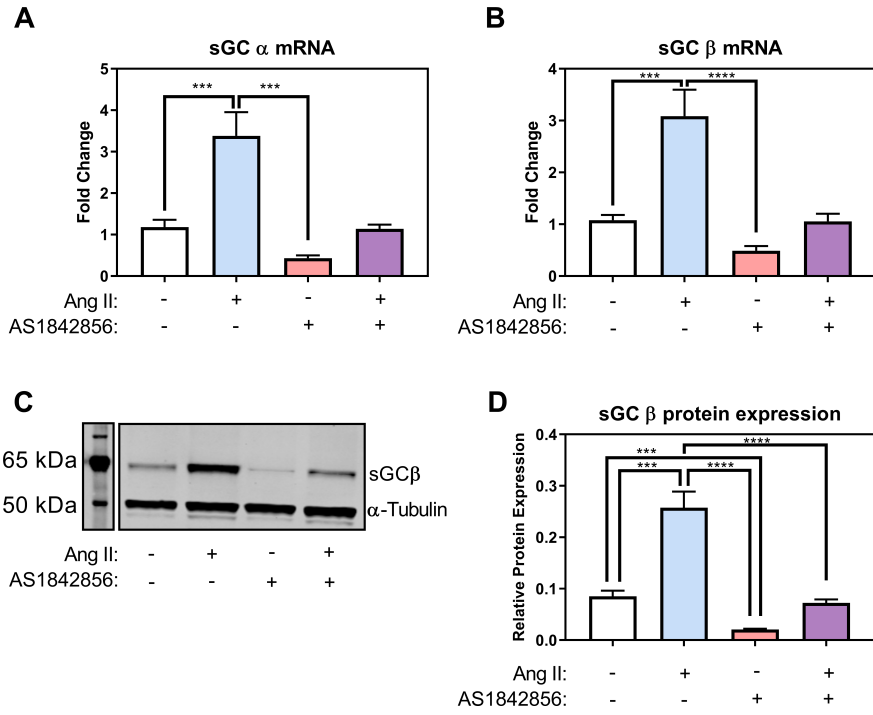
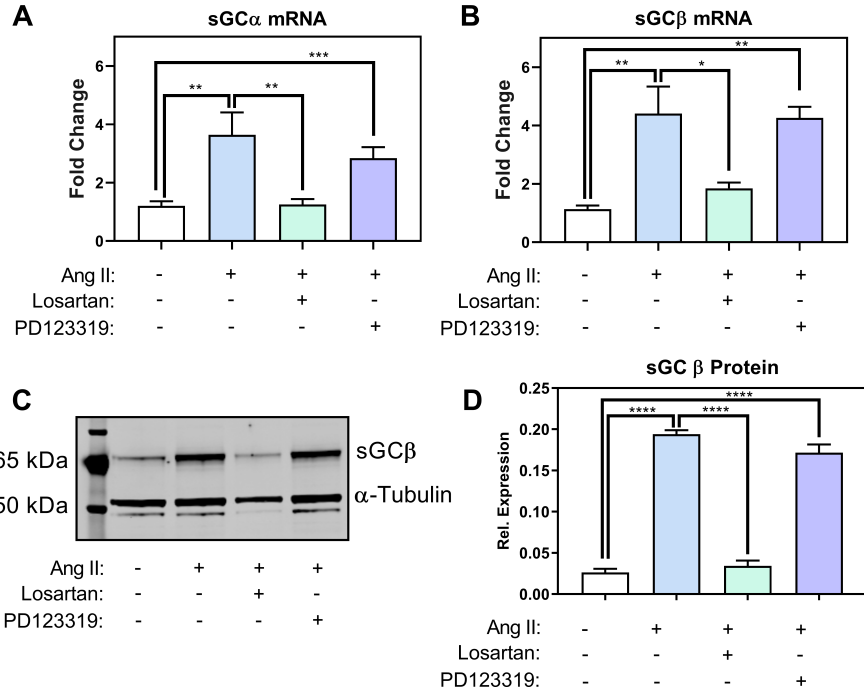
Zhang Y, Griendling KK, Dikalova A, Owens GK, & Taylor WR (2005). Vascular hypertrophy in angiotensin II-induced hypertension is mediated by vascular smooth muscle cell-derived H₂O₂. *Hypertension* 46:732-737.

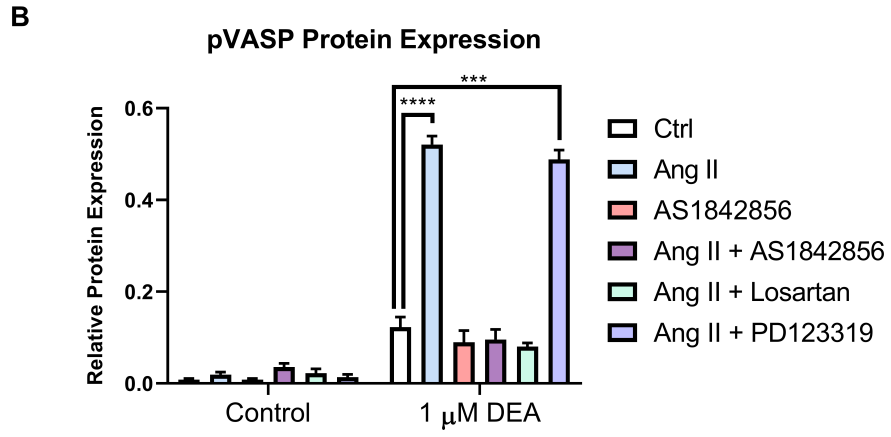
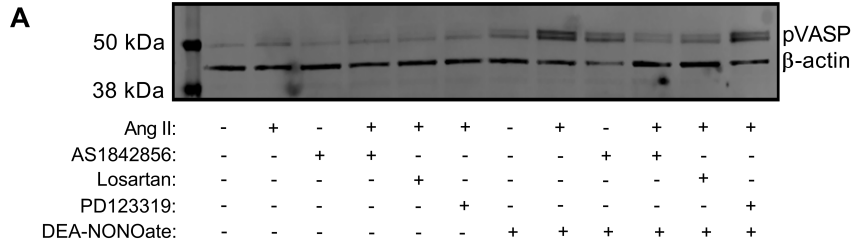
Zhu X, & Jackson EK (2017). RACK1 regulates angiotensin II-induced contractions of SHR preglomerular vascular smooth muscle cells. *Am J Physiol Renal Physiol* 312: F565-F576.











Antibody	Species	Application	Concentration	Company	Cat. Number
sGC β	rabbit	WB, IHC, ICC	1:1000, 1:100, 1:200	Cayman	160897
β -actin	mouse	WB	1:500	Sigma	
α -tubulin	mouse	WB	1:10000	Sigma	T6074
Anti-rabbit Alexafluor-594	donkey	IHC, ICC	1:250, 1:250	Life Technologies	A21207
Goat Alexafluor-647	donkey	IHC	1:250	Life Technologies	A21447
ACTA2 conjugated Alexafluor-488	mouse	IHC	1:250	Sigma	F3777
Von Willebrand Factor	sheep	IHC	1:100	Abcam	ab11713
Rabbit IgG	rabbit	IHC	1:250	Vector Laboratories	I-1000

Primer	Sequence
Rat sGC α F	CTC CCG TGA CCG CAT CAT
Rat sGC α R	CCG GTG TTG ATG TTG ACT GA
Rat sGC β F	AAT TAC GGT CCC GAG GTG TG
Rat sGC β R	GCA GCA GCC ACC AAG TCA TA
Mammalian 18S F	ACG GAC AGG ATT GAC AGA TTG
Mammalian 18S R	TTA GCA TGC CAG AGT CTC GTT